

Interacting Molecular Loops in the Mammalian Circadian Clock

Lauren P. Shearman,^{1*} Sathyanarayanan Sriram,^{1*}
David R. Weaver,¹ Elizabeth S. Maywood,²
Inês Chaves,³ Binhai Zheng,⁴ Kazuhiko Kume,¹
Cheng Chi Lee,⁴ Gijsbertus T. J. van der Horst,³
Michael H. Hastings,² Steven M. Reppert^{1†}

We show that, in the mouse, the core mechanism for the master circadian clock consists of interacting positive and negative transcription and translation feedback loops. Analysis of *Clock/Clock* mutant mice, homozygous *Period2^{Brdm1}* mutants, and *Cryptochrome*-deficient mice reveals substantially altered *Bmal1* rhythms, consistent with a dominant role of PERIOD2 in the positive regulation of the *Bmal1* loop. In vitro analysis of CRYPTOCHROME inhibition of CLOCK:BMAL1-mediated transcription shows that the inhibition is through direct protein:protein interactions, independent of the PERIOD and TIMELESS proteins. PERIOD2 is a positive regulator of the *Bmal1* loop, and CRYPTOCHROMES are the negative regulators of the *Period* and *Cryptochrome* cycles.

Circadian clock-controlled rhythms provide an orchestrated temporal program that allows for the appropriate timing of physiology and behavior, optimizing the efficiency of biological systems. In mammals, a master clock generating circadian rhythms is located in the suprachiasmatic nuclei (SCN) of the hypothalamus (1, 2). Synchronization of the multiple, cell-autonomous circadian clocks within the SCN leads to coordinated circadian outputs that regulate expressed rhythms (3–7).

In its simplest form, the molecular clockwork consists of autoregulatory transcriptional and translational feedback loops that have both positive and negative elements (8). The positive components are two basic helix-loop-helix, PAS domain-containing transcription factors, CLOCK and BMAL1 (9–11). When these transcription factors heterodimerize, they drive the transcription of three *Period* genes (in the mouse, designated *mPer1*, *mPer2*, and *mPer3*) and two *Cryptochrome* genes (*mCry1* and *mCry2*) (9, 12, 13). The mPER and mCRY proteins appear to act as negative components of the feedback loop. By in vitro luciferase reporter gene assays, each protein can negatively regulate CLOCK:BMAL1-mediated transcription through CACGTG E box enhancer elements (12–14).

The mouse *Timeless* (*mTim*) protein,

which can also negatively regulate CLOCK:BMAL1-mediated transcription in vitro (12, 14), is constitutively expressed in the nucleus of most SCN neurons (15). Unlike TIM in *Drosophila*, however, mTIM does not translocate the mPER proteins from cytoplasm to nucleus (13), nor is it light responsive (16). In fact, recent database entries show that the *mTim* is not the true mammalian homolog of *Drosophila tim* (17).

Mutations of *Clock* (*clk*, a 51-amino acid deletion from the putative transcriptional activation domain) cause abnormally long circadian periods in behavior, with homozygous mutant mice eventually becoming arrhythmic in constant darkness (DD) (18, 19). The dominant negative, mutant CLOCK protein can still form heterodimers with BMAL1 that bind to DNA but cannot activate transcription (9). Consistent with this deficiency, the RNA rhythms of *mPer1*, *mPer2*, *mPer3*, and *mCry1* are all significantly blunted in the SCN of homozygous *Clk* mutant mice (12, 13, 20). In addition, *mCry2* RNA levels, which are not expressed in a circadian rhythm in the SCN in our hands (21), are significantly depressed in *Clk/Clk* mice (13), as are the RNA rhythms of two clock-controlled genes (CCGs), vasopressin preproressophysin and albumin D-element binding protein (12, 20, 22, 23).

Mice lacking both *mCry1* and *mCry2*, however, exhibit a complete loss of circadian rhythmicity in wheel running behavior immediately upon placement in DD (24, 25). *mPer1* and *mPer2* RNA levels are arrhythmic and expressed at tonic mid-to-high values in the SCN, consistent with a nonfunctioning circadian clock (21, 25). This finding is also consonant with in vitro studies showing that the mCRY proteins are potent inhibitors of CLOCK:BMAL1-mediated transcription (13), so that in

their absence, expression of genes driven by CLOCK:BMAL1 is enhanced.

The behavioral and molecular phenotypes of *mPer2* mutant animals are more complex. In the protein coded by the mutant *mPer2* allele (*mPer2^{Brdm1}*), 87 residues are missing from the carboxyl portion of the PAS dimerization domain (26). Homozygous *mPer2^{Brdm1}* mutant mice show a shorter circadian period followed by loss of circadian rhythmicity in DD. *mPer1* and *mPer2* RNA levels are still rhythmic in the SCN of homozygous mutants on initial placement in DD, but the rhythms are severely reduced in amplitude because of reduced peak RNA levels (26). The molecular phenotype of the mutant mice is surprising, because reduced RNA levels are not consistent with a potent role of mPER2 in its own negative regulation or the negative regulation of the *mPer1* RNA oscillation. Instead, the molecular phenotype of the *mPer2^{Brdm1}* mutation is consistent with strong positive regulatory function of mPER2 in the core clock mechanism (26).

The discrepancy between the molecular alterations in *mCry*-deficient mice and homozygous *mPer2^{Brdm1}* mutant animals could be explained by the existence of another interdigitating clock feedback loop, similar to a scheme proposed in *Drosophila* (27). In the mouse, this other loop would involve the rhythmic regulation of *Bmal1*, because *Clk* RNA levels do not oscillate (28, 29). *Bmal1* RNA is indeed rhythmic in the SCN of rats and mice with a phase opposite that of *Per1* and *Per2* (20, 30, 31). Because mPER1, mPER2, mCRY1, and mCRY2 exhibit synchronous oscillations of nuclear localization in the SCN (13, 16), the proteins could be simultaneously negatively regulating their own transcription and positively regulating the transcription of *Bmal1*.

We now provide evidence for an interdigitating *Bmal1* feedback loop in the mouse SCN and suggest that the dynamically regulated mPER and mCRY proteins have differential effects, with mCRYs being predominantly negative regulators of the *mPer* and *mCry* cycles and the mPER2 protein being a dominant positive regulator of the *Bmal1* loop.

Bmal1 RNA rhythm in *Clk/Clk* mice.

We first documented a *Bmal1* RNA rhythm in mouse SCN using in situ hybridization (32) with an antisense riboprobe to the two major *Bmal1* transcripts in the SCN (33, 34). Wild-type mice exhibited a robust circadian rhythm in *Bmal1* RNA levels (Fig. 1A), with low levels from circadian time (CT) 6 to 9 and peak levels from CT 15 to 18.

The phase of the *Bmal1* rhythm is opposite that of the *mPer1*, *mPer2*, and *mPer3* RNA rhythms (35), as reported (20, 30, 31). In addition to driving rhythmic transcription of the *mPer* and *mCry* genes (12, 13), it seemed possible that CLOCK:BMAL1 het-

¹Laboratory of Developmental Chronobiology, Mass-
General Hospital for Children, Massachusetts General
Hospital, and Harvard Medical School, Boston, MA
02114, USA. ²Department of Anatomy, University of
Cambridge, Downing Street, Cambridge CB2 3DY, UK.
³Medical Genetic Center, Department of Cell Biology
and Genetics, Erasmus University, 3000 DR Rotter-
dam, Netherlands. ⁴Department of Molecular and Hu-
man Genetics, Baylor College of Medicine, One Baylor
Plaza, Houston, TX 77030, USA.

*These authors contributed equally to this work.

†To whom correspondence should be addressed. E-
mail: reppert@helix.mgh.harvard.edu

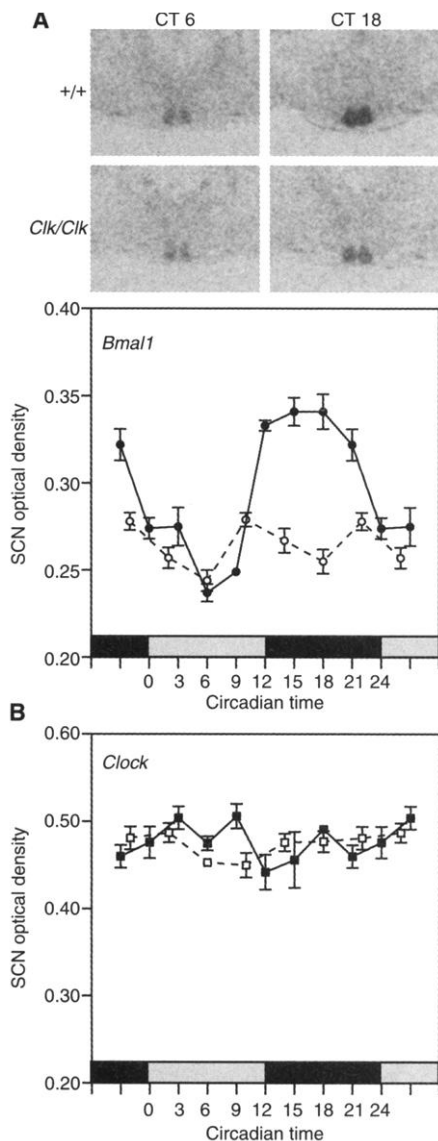


Fig. 1. *Bmal1* and *Clock* RNA levels are differentially altered in *Clock/Clock* mutant (*Clk/Clk*) mice. **(A)** *Bmal1* RNA levels are reduced in the SCN of *Clk/Clk* mice [significant difference between genotypes; analysis of variance (ANOVA), $P < 0.001$]. (Top) Representative autoradiograms of coronal brain sections at the level of the SCN from wild-type (+/+) and *Clk/Clk* mice. In situ hybridization with an antisense cRNA probe was used to detect *Bmal1* RNA. Magnification, $\times 9.4$. (Bottom) Temporal profiles of *Bmal1* RNA levels in the SCN of wild-type (solid) and *Clk/Clk* (dashed) mice are depicted. Each value is the mean \pm SEM of five to nine animals. Data at CT 2, 3, 22, and 24 are double-plotted. Gray bar, subjective day; black bar, subjective night. **(B)** *Clk* RNA levels are not altered in the SCN of *Clk/Clk* mice (ANOVA, $P > 0.05$). Expression of *Clk* mRNA was not rhythmic in the SCN of wild-type (solid line) or *Clk/Clk* (dashed line) mice. In situ hybridization with an antisense cRNA probe was used to detect *Clk* RNA (nucleotides 1343 to 1831 of accession number AF000998). Each value is the mean \pm SEM of five to nine animals. Double plotting and lighting cycle as in (A).

erodimers might simultaneously negatively regulate *Bmal1* gene expression, as proposed for CLK regulation in *Drosophila* (27). If CLOCK:BMAL1 heterodimers negatively regulate *Bmal1* gene expression and if the mutant CLOCK protein is ineffective in this activity, then *Bmal1* RNA levels should be elevated and less rhythmic in homozygous *Clock* mutant (*Clk/Clk*) mice (36). Compared with wild types, however, *Clk/Clk* animals expressed a severely dampened circadian rhythm of *Bmal1* RNA levels in the SCN (Fig. 1A), as reported previously (20). Trough *Bmal1* RNA levels did not differ between *Clk/Clk* mice and wild types. The peak level of the RNA rhythm in homozygous *Clk* mutant mice was only $\approx 30\%$ of the peak value in wild types.

We also examined the temporal profile of *Clk* RNA levels in the SCN of *Clk/Clk* mutant animals, because it has been reported that *Clk* RNA levels (assessed by Northern blot analysis) are decreased in the eye and hypothalamus of *Clk/Clk* mutant mice (19). Consistent with previous reports (28, 29), *Clk* RNA levels did not manifest a circadian oscillation in mouse SCN (Fig. 1B). *Clk* RNA levels in the SCN of *Clk/Clk* mutant mice were not significantly different from those in the SCN of wild-type animals (Fig. 1B). Thus, the *Clk* mutation appears to alter regulation of *Bmal1* gene expression in SCN, but not the regulation of the *Clk* gene itself. *Clk* expression may be decreased in other hypothalamic regions.

The low levels of *Bmal1* RNA in the SCN of homozygous *Clk* mutant animals show that CLOCK is not required for the negative regulation of *Bmal1*. Instead, these data indicate that CLOCK is actually necessary for the positive regulation of *Bmal1*. The positive effect of CLOCK on *Bmal1* levels is probably indirect and may occur through the mPER and/or mCRY proteins, which are expressed in the nucleus of SCN neurons at the appropriate circadian time to enhance *Bmal1* gene expression (13, 15, 16). In addition, the *mPer1*, *mPer2*, *mPer3*, *mCry1*, and *mCry2* RNA oscillations are all down-regulated in *Clk/Clk* mutant mice (12, 13). Reduced levels of the protein products of one or more of these genes may lead to the reduced levels of *Bmal1* in the mutant mice, through loss of a positive drive on *Bmal1* transcription.

***Bmal1* and *mCry1* RNA rhythms in *mPer2^{Brdm1}* mutant mice.** Homozygous *mPer2^{Brdm1}* mutant animals have depressed *mPer1* and *mPer2* RNA rhythms (26). We thus examined the *Bmal1* rhythm in homozygous *mPer2^{Brdm1}* mutants to determine whether the positive drive on the *Bmal1* feedback loop might come from the mPER2 protein. We also examined the effects of this mutation on the *mCry1* RNA rhythm.

The temporal profiles of gene expression were analyzed at six time points over the first

day in DD in homozygous *mPer2^{Brdm1}* mutant mice and wild-type littermates (37). The *Bmal1* RNA rhythm in the SCN of wild-type animals was substantially different than that of mutant mice (Fig. 2A). Trough RNA levels did not differ between wild-type and mutant animals, but the increase in *Bmal1* RNA levels was advanced and truncated in the mutants, compared with the wild-type rhythm.

The *mCry1* RNA rhythm was also significantly altered. In the SCN of *mPer2^{Brdm1}* mutant mice (Fig. 2B), the peak levels of the *mCry1* RNA rhythm were suppressed by $\approx 50\%$, as reported for *mPer1* and *mPer2* RNA rhythms in this mouse line (26).

These data suggest that maintenance of a normal *Bmal1* RNA rhythm is important for the positive transcriptional regulation of the *mPer* and *mCry* feedback loops. Thus, rhythmic *Bmal1* RNA levels may drive rhythmic BMAL1 levels, which, in turn, regulate CLOCK:BMAL1-mediated transcriptional enhancement in the master clock. Indeed, *mPer1*, *mPer2*, and *mCry1* RNA rhythms are all blunted in the SCN of *mPer2^{Brdm1}* mutant mice, in which the *Bmal1* rhythm is also blunted [(26) and present data]. In addition, the homozygous *mPer2^{Brdm1}* mutation is associated with a shortened circadian period and ensuing arrhythmicity in DD (26).

These data, along with the fact that *Clk* RNA levels are unaltered in the SCN of homozygous *mPer2^{Brdm1}* mutants (26), also provide evidence that mPER2 is a positive regulator of the *Bmal1* RNA rhythm. This effect may be unique to mPER2. For example, the diurnal oscillation in *mPer2* RNA is not altered in the SCN of *mPer1*-deficient mice (38), and *mPer1*, *mPer2*, and *Bmal1* RNA circadian rhythms are not altered in the SCN of *mPer3*-deficient mice (39). Moreover, circadian rhythms in behavior are sustained in mice deficient in either *mPer1* or *mPer3* (38, 39).

mCRY-mediated nuclear translocation of mPER2. There are at least two ways that the *mPer2^{Brdm1}* mutation could alter the positive drive of the clock feedback loops. The mutation could disrupt mPER:mCRY interactions important for the synchronous oscillations of their nuclear localization and/or alter the protein's ability to interact with other proteins (e.g., transcription factors). We examined whether the PAS domain is necessary for functionally relevant mPER2:mCRY interactions using immunofluorescence of epitope-tagged proteins in COS-7 cells (40).

Coexpression of mPER1 or mPER2 with either mCRY1 or mCRY2 in COS-7 cells translocates $>90\%$ of mPER1 and mPER2 into the nucleus (13). To determine whether the PAS domain of mPER2 is required for this translocation, residues 1 to 434 (mPER2¹⁻⁴³⁴), which include the PAS domain, were examined in COS-7 cells. mPER2¹⁻⁴³⁴ was localized to both

cytoplasm and nucleus (89% of transfected cells) (Fig. 3), and the localization was not changed by coexpression with mCRY1. Coexpression of mPER2⁴³⁵⁻¹²⁵⁷ with mCRY1, however, markedly changed the cellular location of the mPER2 fragment from cytoplasm only (84%) to nucleus only (85%). Coexpression of mPER2^{Brdm1} (missing residues 348 to 434) with mCRY1 also moved mutant mPER2 into the nucleus, from cytoplasm only (100% when expressed alone) to predominantly both cytoplasm and nucleus (81%) (Fig. 3). The same patterns of cellular localization were found when mCRY2 was coexpressed with these mPER2 constructs. Thus, functional mPER2: mCRY interactions are not mediated through the PAS domain. Similarly, the PAS domain was not important for the mCRY-mediated nuclear translocation of mPER1 in COS-7 cells (41).

Because the mPER:mCRY interactions necessary for nuclear transport occur outside the PAS region, the PAS domain of an mPER2:mCRY heterodimer might be free to bind to an activator (e.g., transcription factor) and shuttle it into the nucleus to activate *Bmal1* transcription. Alternatively, once in the nucleus, mPER2:mCRY heterodimers or mPER2 monomers could coactivate *Bmal1*

transcription through a PAS-mediated interaction with a transcription factor (27). mPER2 itself does not have a DNA-binding motif (42).

Bmal1 RNA levels in mice lacking mCry1 and mCry2. The tonic mid-to-high *mPer1* and *mPer2* RNA levels in *mCry*-deficient mice (21) suggest that CLOCK:BMAL1 heterodimers might be constantly driving *mPer1* and *mPer2* gene expression in the absence of transcriptional inhibition by the mCRY proteins. To examine whether *Bmal1* RNA levels would also be modestly elevated, we compared *Bmal1* RNA levels in the SCN of *mCry*-deficient mice with those in the SCN of wild-type mice of the same genetic background at CT 6 and at CT 18 (43). We also examined *Clk* RNA levels in these animals.

In wild-type animals, the typical circadian variation in *Bmal1* RNA levels was apparent with high levels at CT 18 and low levels at CT 6 (Fig. 4A). In *mCry*-deficient mice, on the other hand, *Bmal1* RNA levels were low at both circadian times (Fig. 4A). *Clk* RNA levels did not differ as a function of circadian time or genotype (Fig. 4B).

The unexpected low *Bmal1* gene expression in the SCN of *mCry*-deficient mice suggests that the *Bmal1* feedback loop is disrupt-

ed in the mutant animals, with a resultant nonfunctional circadian clock. Nevertheless, enough *Bmal1* gene expression and protein synthesis occur for heterodimerization with CLOCK so that, without the strong negative feedback normally exerted by the mCRY proteins, *mPer1* and *mPer2* gene expression is driven sufficiently by the heterodimer to give intermediate to high RNA values (depending on RNA stability).

mPER1 and mPER2 localization in mCry-deficient mice. The mid-to-high *mPer1* and *mPer2* RNA levels in the SCN of *mCry*-deficient mice and simultaneous low *Bmal1* levels suggest that mPER1 and mPER2 proteins may not be exerting much positive or negative influence on the core feedback loops. To test this, we determined whether mPER1 and mPER2 were tonically expressed in the nuclei of SCN cells in *mCry*-deficient mice, because nuclear location appears necessary for action on transcription (13, 16).

mPER1 immunoreactivity exhibited a robust rhythm of nuclear staining in the SCN of wild-type mice, with high values at CT 12 (328 ± 3.5, mean ± SEM of positive nuclei per 30 μm section, n = 3) (Fig. 5A) and significantly lower values at CT 24 (54 ± 5, n = 3; P < 0.01) (Fig. 5B), as reported in other strains of mice (15, 16).

In *mCry*-deficient mice, however, mPER1 immunoreactivity was detected in the nucleus of a similar number of SCN neurons at each of the two circadian times (CT 12, 140 ± 9, n = 3; CT 24, 152 ± 21, n = 3) (Fig. 5, C and D), and the values at each time were at

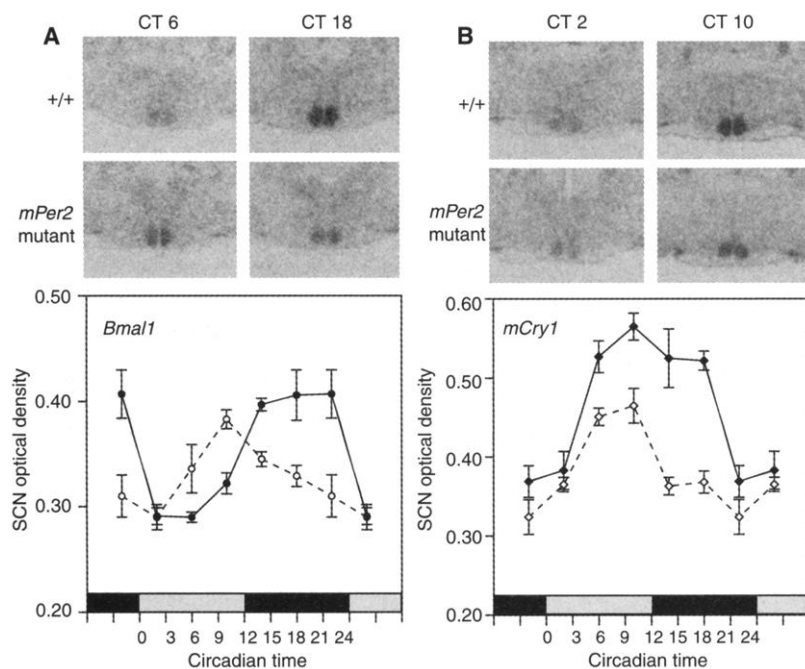


Fig. 2. *Bmal1* and *mCry1* RNA rhythms are blunted in homozygous *mPer2^{Brdm1}* mutant mice. (A) *Bmal1* RNA levels in the SCN of *mPer2^{Brdm1}* mutant mice. (Top) Representative autoradiographs from wild-type (+/+) and homozygous *mPer2^{Brdm1}* (*mPer2* mutant) mice. Magnification, ×9.4. (Bottom) Temporal profiles of *Bmal1* RNA levels in the SCN of wild-type (solid line) and *mPer2* mutant (dashed line) mice, as in Fig. 1 (significant difference between genotypes; ANOVA, P < 0.05). Each value is the mean ± SEM of four animals. (B) *mCry1* RNA levels in the SCN of *mPer2^{Brdm1}* mutant mice. (Top) Representative autoradiographs from wild-type (+/+) and homozygous *mPer2^{Brdm1}* mice. In situ hybridization with an antisense cRNA probe was used to detect *mCry1* RNA (nucleotides 1081 to 1793 of accession number AB000777). Magnification, ×9.4. (Bottom) Temporal profiles of *mCry1* RNA levels in the SCN of wild-type (solid line) and *mPer2* mutant (dashed line) mice are shown, as in Fig. 1 (significant difference between genotypes; ANOVA, P ≤ 0.0001). Each value is the mean ± SEM of four animals.

	-mCRY1		+mCRY1			
	C	B	N	C		B
mPER2 ¹⁻¹²⁵⁷	67	33	0	0	2	98
mPER2 ¹⁻⁴³⁴	9	89	2	9	91	0
mPER2 ⁴³⁵⁻¹²⁵⁷	84	8	8	12	3	85
mPER2 ^{Brdm1}	100	0	0	9	81	10

Fig. 3. mPER2:mCRY interactions occur independently of the PAS domain. Location of immunofluorescence of V5-tagged mPER2 constructs expressed in COS-7 cells with (+) or without (-) mCRY1. The mPER2^{Brdm1} construct was generated by overlap extension polymerase chain reaction. All constructs were confirmed by sequence analysis. The V5 epitope was at the COOH-terminus. The cellular location of immunofluorescence was scored as cytoplasm only (C), both cytoplasm and nucleus (B), or nucleus only (N). Values shown are the mean percentages from two experiments; all values were within 17% of the mean. Gray bars, PAS domain.

≈40% of those seen at peak (CT 12) in wild-type animals.

The double *mCry* mutation also altered the subcellular distribution of mPER1 staining in the SCN. In wild-type mice, mPER1 staining viewed under contrast interference was nuclear with a very condensed immunoreaction and a clear nucleolus (Fig. 5E, arrow). The neuropil of the SCN in wild types was devoid of mPER1 immunoreactivity. In the SCN of *mCry*-deficient animals, mPER1 staining was nuclear (Fig. 5F, solid arrow), but the nuclear profiles were less well defined and less intensely stained, and perinuclear, cytoplasmic immunoreaction could be observed (Fig. 5F, open arrow). In addition, the neuropil staining for mPER1 was higher in *mCry*-deficient mice, although dendritic profiles were not discernible. In the same brains, the constitutive nuclear staining for mPER1

normally seen in the piriform cortex was not altered in *mCry*-deficient animals (Fig. 5, G and H).

mPER2 immunoreactivity also exhibited a robust rhythm of nuclear staining in the SCN of wild-type mice, with high values at CT 12 (371 ± 11 , $n = 3$) (Fig. 5A') and significantly lower counts at CT 24 (31 ± 3 , $n = 3$; $P < 0.01$) (Fig. 5B'), as reported in another strain (16). In contrast, the pattern of mPER2 immunoreactivity in the SCN of *mCry*-deficient mice was markedly altered, with few mPER2 immunoreactive cells in the SCN of *mCry*-deficient animals at either circadian time (CT 12, 12 ± 1 , $n = 3$; CT 24, 8 ± 2 , $n = 3$; Fig. 5, C' and D').

In the wild-type mice, the mPER2 staining profiles were nuclear, with well-defined outlines and nucleoli devoid of reaction product (Fig. 5E', arrow). In the few mPER2 immunoreactive cells in the SCN of *mCry*-deficient mice, low-level mPER2 staining was observed in the nucleus (Fig. 5F'), but

the profiles were poorly defined and low-intensity perinuclear staining could also be observed (open arrow). As for mPER1, genotype had no discernible effect on nuclear mPER2 immunoreactivity in the piriform cortex (Fig. 5, G' and H'), although there was evidence of a low level of perinuclear immunoreactivity for mPER2 (Fig. 5H', arrows) in piriform cortex of *mCry*-deficient mice.

The marked reduction of mPER2 staining in the SCN of *mCry*-deficient animals suggests that the mCRY proteins are either directly or indirectly important for mPER2 stability, as *mPer2* RNA levels are at tonic intermediate to high levels in *mCry*-deficient mice, similar to those found for *mPer1* RNA levels (21). It seems unlikely that we are not detecting mPER2 in the cytoplasm of *mCry* mutants, because antibody to mPER2 can detect cytoplasmically localized antigen in SCN cells (16).

The low levels of mPER2 immunoreactivity in the SCN of *mCry*-deficient mice, in

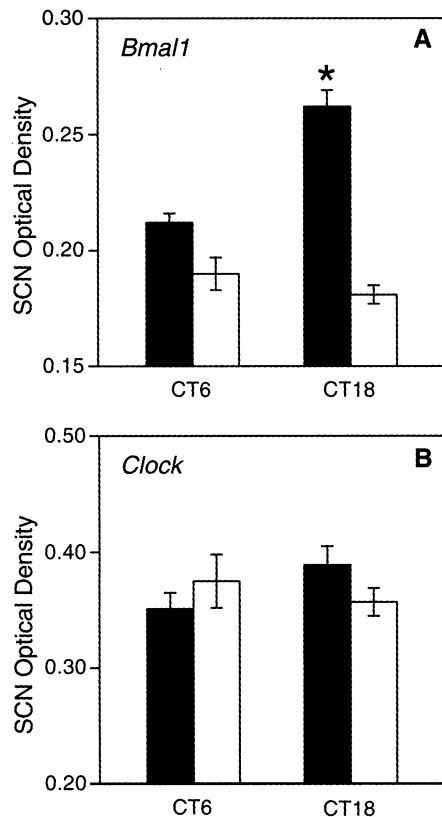


Fig. 4. *Bmal1* and *Clk* RNA levels are differentially regulated in *mCry*-deficient mice. (A) Attenuated peak levels of *Bmal1* RNA in *mCry*-deficient mice. Quantitation of *Bmal1* RNA levels in the SCN of wild-type (solid bars) and *mCry*-deficient (open bars) mice. Values are the mean \pm SEM of five animals. Mice were studied on the first day in DD. *, significant difference in wild-type mice, $P < 0.001$; there was no significant difference in *mCry*-deficient mice, $P > 0.05$. (B) *Clk* gene expression in the SCN of *mCry*-deficient mice. Quantitation of *Clk* RNA levels in the SCN of wild-type (solid bars) and *mCry*-deficient (open bars) mice showed no differences ($P > 0.05$). Values are the mean \pm SEM of five animals.

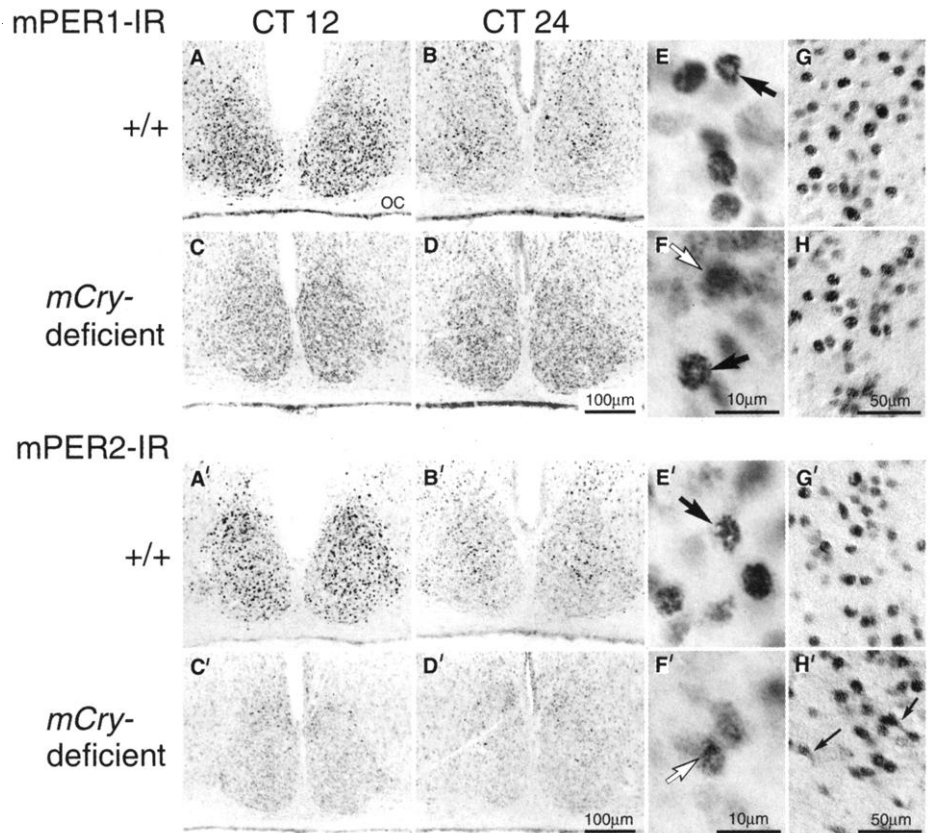


Fig. 5. The intracellular location of mPER1 and mPER2 is altered in the SCN of *mCry*-deficient mice. (Top panels) mPER1 immunoreactivity (mPER1-IR) in the SCN and piriform cortex of wild-type (+/+) and *mCry*-deficient mice. (A and B) Representative coronal sections of the SCN in wild-type mice at CT12 (A) and CT 24 (B). (C and D) Expression in *mCry*-deficient mice at CT12 (C) and CT24 (D). OC, optic chiasm. (E and F) High-power contrast interference views of SCN from wild-type (E) and *mCry*-deficient (F) mice. (G and H) Nuclear mPER1-IR in the piriform cortex of wild-type (G) and mutant (H) mice. (Bottom panels) mPER2 immunoreactivity (mPER2-IR) in the SCN and piriform cortex of wild-type (+/+) and *mCry*-deficient mice. (A' and B') Representative coronal sections in the SCN of wild-type mice at CT12 (A') and CT 24 (B'). (C' and D') Expression in *mCry*-deficient mice at CT12 (C') and CT24 (D'). (E' and F') High-power contrast interference views of SCN from wild-type mice (E') and *mCry*-deficient mice (F'). (G' and H') mPER2-IR in the piriform cortex in wild-type (G') and mutant (H') mice.

conjunction with tonically low *Bmal1* RNA levels, are consistent with an important role of mPER2 in the positive regulation of the *Bmal1* loop. Because mPER1 is present in SCN nuclei in *mCry*-deficient mice yet *Bmal1* RNA is low, mPER1 likely has little effect on the positive regulation of the *Bmal1* feedback loop or negative regulation of the *mPer1*, *mPer2*, and *mPer3* cycles.

mPER1 and mPER2 can each enter the nucleus even in the absence of mCRY:mPER interactions. mPER1 is expressed in the nucleus of SCN neurons from *mCry*-deficient mice, and both mPER1 and mPER2 are constitutively expressed in the nucleus of cells in the piriform cortex of *mCry*-deficient animals. The phosphorylation state of mPER1 dictates its cellular location in the absence of mPER1:mCRY interactions, because its phosphorylation by casein kinase I epsilon leads to cytoplasmic retention in vitro (44). Thus, the nuclear location of both mPER1 and mPER2 in vivo may depend on several factors, including interactions with mCRY and other proteins and their phosphorylation.

mCRY-induced inhibition of transcription. The intermediate to high levels of *mPer1* and *mPer2* gene expression throughout the circadian day in *mCry*-deficient mice (21, 25) are consistent with a prominent role of the mCRY proteins in negatively regulating CLOCK:BMAL1-mediated transcription, as in vitro data have suggested (13). The endogenous expression of the *mCry1*, *mCry2*, *mPer1*, *mPer2*, and *mPer3* genes in mammalian cell lines, however, has obscured rigorous in vitro analysis of the mechanism. Therefore, we used an insect cell line, Schneider (S2) cells, a *Drosophila* cell line that expresses *cycle* (the *Drosophila Bmal1*) but not *per*, *tim*, and *clock* (45, 46), to study the negative regulation of mCRY1 and mCRY2 on E box-mediated transcription. The luciferase reporter consists of a tandem repeat of the *Drosophila per* E box (CACGTG) and flanking nucleotides fused to *hsp70* driving luciferase (46, 47).

Because S2 cells express endogenous *cyc*, transfection with *dclock* alone caused a large increase in transcriptional activity (265-fold) (Fig. 6A), as described (46). As for dCRY (48, 41), this activation was not inhibited by either mCRY1 or mCRY2. When cotransfected, mouse (m)CLOCK and syrian hamster (sh)BMAL1 heterodimers induced a large increase in transcriptional activity (1744-fold) that was reduced by >90% by mCRY1 or mCRY2 (Fig. 6A). Moreover, cotransfection of *shBmal1* and human (*h*)*Mop4* (49), but not transfection of *hMop4* alone, similarly caused a large increase in transcriptional activity in S2 cells (539-fold), like that previously found for hMOP4:shBMAL1 heterodimers in mammalian cells (10, 13). hMOP4:shBMAL1-mediated transcription was also blocked by either mCRY1 or mCRY2 (Fig. 6A). The mCLOCK:

shBMAL1- and hMOP4:shBMAL1-induced transcription in S2 cells was dependent on an intact CACGTG E box, because neither heterodimer caused an increase in transcription when a mutated E box reporter was used in the transcriptional assay (41). Immunofluorescence of epitope-tagged mCRY1 or mCRY2 expressed in S2 cells showed that each was >90% nuclear in location, as in mammalian cells (13).

These data indicate that mCRY1 and mCRY2 are nuclear proteins that can each inhibit mCLOCK:shBMAL1-induced transcription independent of the mPER and mTIM proteins and of each other. The results also show that the inhibitory effect is not mediated by the interaction of either mCRY1 or mCRY2 with the E box itself, because E box-mediated transcription was not blocked by the mCRY proteins when transcription was activated by dCLOCK:CYC heterodimers. It thus appears that the mCRY proteins inhibit mCLOCK:shBMAL1-mediated transcription by interacting with either or both of the transcription factors, because a similar inhibition was found with hMOP4:shBMAL1-induced transcription. Yeast two-hybrid assays (50) revealed strong interactions of each mCRY protein with

mCLOCK and shBMAL1 (Fig. 6B). Weaker interactions were detected between each mCRY protein and hMOP4. This is further evidence of functionally relevant associations of each mCRY protein with each of the three transcription factors (51).

We next tried to determine whether the mCRY-induced inhibition of transcription was through interaction with CLOCK and/or BMAL1. Because neither mCRY1 or mCRY2 inhibited dCLOCK:CYC-mediated transcription, we examined the ability of each to inhibit dCLOCK:shBMAL1-mediated transcription. This aspect of study could not be examined in S2 cells because of the strong activation induced by transfecting *dclock* alone in S2 cells where there is strong endogenous *cyc* expression (52). mCRY1 and mCRY2 completely inhibited mCLOCK:shBMAL1- and hMOP4:shBMAL1-induced transcription in COS-7 cells (Fig. 6C, left and middle, respectively), whereas the cryptochromes did not inhibit dCLOCK:shBMAL1-mediated transcription by more than 20% (Fig. 6C, right). Thus, mCRY inhibits mCLOCK:shBMAL1-induced transcription through interaction with either mCLOCK alone or through

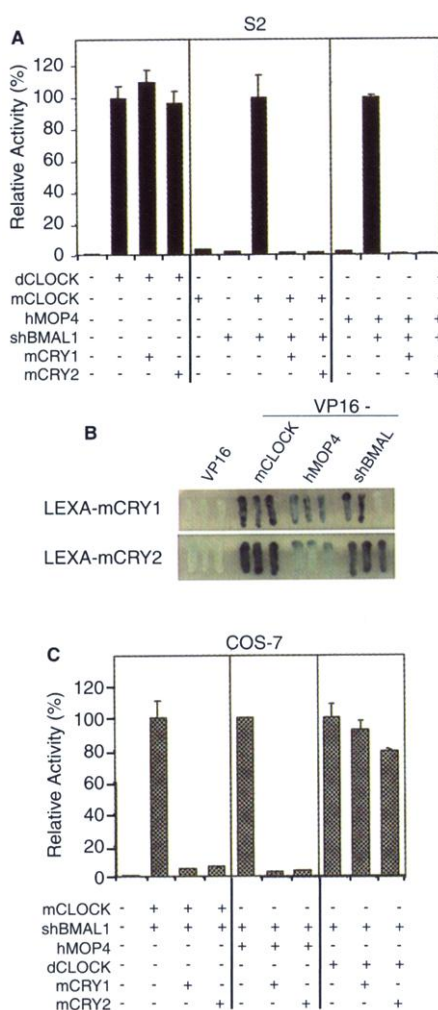
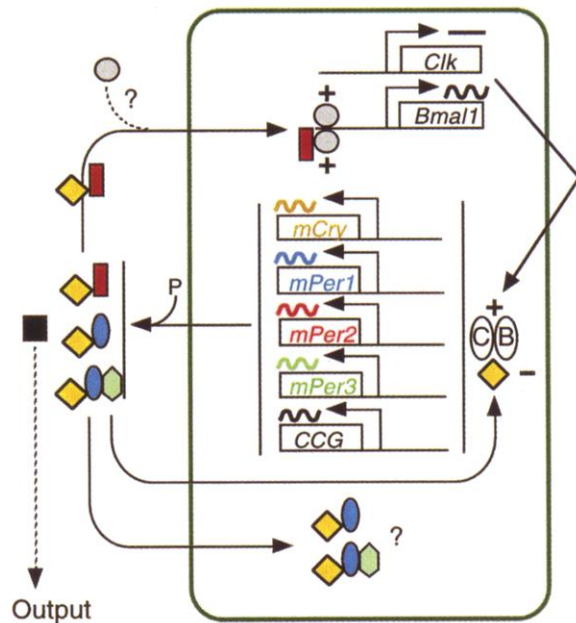


Fig. 6. mCRY-induced inhibition of transcription occurs independently of the mPER and mTIM proteins. **(A)** Effects of mCRY proteins on transcriptional activation in *Drosophila* S2 cells. The luciferase reporter contains four copies of a *Drosophila per* E box and flanking nucleotides fused to *hsp70* driving luciferase (48). Presence (+) or absence (-) of reporter and expression plasmids (1 ng of *dclock*; 50 ng of *mClock*, *shBmal1*, and *hMop4*; 100 ng of *mCry1* and *mCry2*) is denoted. Values are luciferase activity expressed as relative to the response in presence of activators (100%). Each value is the mean \pm SEM of three replicates from a single assay. The results shown are representative of three independent experiments. **(B)** Yeast two-hybrid assays showing mCRY interactions with mCLOCK, hMOP4, and shBMAL1. Patches of yeast are shown expressing LEXA baits with VP16 transactivation hybrids. The blue color indicates β -Gal activity of protein: protein-induced activation of *lacZ* reporter gene. Triplicate patches are from three independent transformants. The same interactions were found in replicate experiments. **(C)** Effects of mCRY proteins on transcriptional activation in COS-7 cells. The luciferase reporter (pGL3-Basic) used contains a 200-base pair fragment of the 5' flanking region of the mouse vasopressin prepropressophysin gene, which includes the endogenous promoter (12). Presence (+) or absence (-) of reporter (10 ng) and expression plasmids (0.25 μ g of *mClock*, *shBmal1*, *hMop4*, and *dclock*; 0.1 μ g of *mCry1* and *mCry2*) is denoted. Values are luciferase activity expressed as relative to the response in presence of activators (100%). Each value is the mean \pm SEM of three replicates from a single assay. The results shown are representative of three independent experiments.

Fig. 7. Model of circadian clockwork within an individual SCN neuron. Gold, mCRY; blue, mPER1; red, mPER2; green, mPER3; black, CCG; gray, hypothetical activator of *Bmal1* transcription. C, CLOCK; B, BMAL1. CLOCK:BMAL1 heterodimers activate (+) rhythmic transcription of *mCry*, *mPer*, and clock-controlled genes (CCG). The mCRY and mPER proteins form complexes important for nuclear translocation of the mPER proteins (13). The phosphorylation (P) state of the mPER proteins may also regulate their cellular location and stability (44, 53, 54). mPER2 positively regulates *Bmal1* transcription by translocating an unidentified activator into the nucleus and/or acting as a coactivator (?). The nuclear-localized mCRY proteins directly interact with CLOCK and BMAL1 to negatively regulate (-) CLOCK:BMAL1-mediated transcription. The functions of nuclear mPER1 and mPER3 have not yet been clearly defined (?). CCGs transduce downstream effects.



an association with both mCLOCK and BMAL1 in a multiprotein complex. Unfortunately, we were unable to examine inhibition of mCLOCK:CYC heterodimers, because co-transfection of *mClock* and *cyc* did not activate transcription in either insect cells (see above) or mammalian cells, even though strong interactions between mCLOCK and CYC were detected in yeast (41).

Molecular organization of the mammalian clockwork. Our working model of the SCN clockwork proposes three types of interacting molecular loops (Fig. 7). The *mCry* genes comprise one loop, with true autoregulatory, negative feedback, in which the protein products feed back to turn off their transcription. The second loop is that manifested by each of the *mPer* genes and some CCGs (for example, vasopressin preproressophysin). This loop type is driven by the same positive elements (CLOCK:BMAL1) as the *mCry* loop, but transcription is not turned off by the respective gene products. Instead, the mCRY protein acts as a negative regulator, leaving the protein products free for other actions. Thus, mPER2 positively drives transcription of the *Bmal1* gene (detailed below), mPER1 may function to stabilize protein components of the loop (16), and CCG products (which might include mPER3) function as output signals (12, 22, 39). The rhythmic regulation of *Bmal1* comprises the third loop with rhythmicity controlled by the cycling presence and absence of a positive element dependent on mPER2. This positive feedback loop augments the positive regulation of the first two loops.

This model of interacting loops proposes that at the start of the circadian day, *mPer* and *mCry* transcription are driven by accumulating CLOCK:BMAL1 heterodimers acting through

E box enhancers. After a delay, the mPER and mCRY proteins are synchronously expressed in the nucleus where the mCRY proteins shut off CLOCK:BMAL1-mediated transcription by directly interacting with these transcription factors. At the same time that the mCRY proteins are inhibiting CLOCK:BMAL1-mediated transcription, mPER2 either shuttles a transcriptional activator into the nucleus or coactivates a transcriptional complex to enhance *Bmal1* transcription (27) (Fig. 7). The importance of the *Bmal1* RNA rhythm is to drive a BMAL1 rhythm after a 4- to 6-hour delay. This delay in the protein rhythm would provide increasingly available CLOCK:BMAL1 heterodimers at the appropriate circadian time to drive *mPer/mCry* transcription, thereby restarting the cycle. We thus predict that BMAL1 availability is rate limiting for heterodimer formation and critical for restarting the loops. Delineating factors that regulate clock protein stability and interactions (phosphorylation and proteolysis) are important next steps for defining how a 24-hour time constant is built into the clockwork (44, 53, 54).

References and Notes

1. D. C. Klein, R. Y. Moore, S. M. Reppert, *Suprachiasmatic Nucleus: The Mind's Clock* (Oxford Univ. Press, New York, 1991).
2. D. R. Weaver, *J. Biol. Rhythms* **13**, 100 (1998).
3. D. K. Welsh, D. E. Logothetis, M. Meister, S. M. Reppert, *Neuron* **14**, 697 (1995).
4. C. Liu, D. R. Weaver, S. Strogatz, S. M. Reppert, *Cell* **91**, 855 (1997).
5. E. D. Herzog, J. S. Takahashi, G. D. Block, *Nature Neurosci.* **1**, 708 (1998).
6. S. Honma, T. Shirakawa, Y. Katsuno, M. Namihira, K. Honma, *Neurosci. Lett.* **250**, 157 (1999).
7. C. Liu and S. M. Reppert, *Neuron* **25**, 123 (2000).
8. J. C. Dunlap, *Cell* **96**, 271 (1999).
9. N. Gekakis et al., *Science* **280**, 1564 (1998).
10. J. B. Hogenesch, Y.-Z. Gu, S. Jain, C. A. Bradfield, *Proc. Natl. Acad. Sci. U.S.A.* **95**, 5474 (1998).
11. S. Takahata et al., *Biochem. Biophys. Res. Commun.* **248**, 789 (1998).
12. X. Jin et al., *Cell* **96**, 57 (1999).
13. K. Kume et al., *Cell* **98**, 193 (1999).
14. A. M. Sangoram et al., *Neuron* **21**, 1101 (1998).
15. M. H. Hastings, M. D. Field, E. S. Maywood, D. R. Weaver, S. M. Reppert, *J. Neurosci.* **19**, RC11 (1999).
16. M. D. Field et al., *Neuron* **25**, 437 (2000).
17. Analysis of the completed *Drosophila* genome has identified a gene of unknown function (encoded on bacterial artificial chromosomes AE003699 and AE003698) that is the structural homolog of *mTim*. A. L. Gotter, L. F. Kolakowski Jr., S. M. Reppert, unpublished data.
18. M. H. Vitaterna et al., *Science* **264**, 719 (1994).
19. D. P. King et al., *Cell* **89**, 641 (1997).
20. K. Oishi, H. Fukui, N. Ishida, *Biochem. Biophys. Res. Commun.* **268**, 164 (2000).
21. H. Okamura et al., *Science* **286**, 2531 (1999).
22. J. A. Ripperger, L. P. Shearman, S. M. Reppert, U. Schibler, *Genes Dev.* **14**, 679 (2000).
23. R. Silver et al., *Neuroreport* **10**, 3165 (1999).
24. G. T. J. van der Horst et al., *Nature* **398**, 627 (1999).
25. M. H. Vitaterna et al., *Proc. Natl. Acad. Sci. U.S.A.* **96**, 12114 (1999).
26. B. Zheng et al., *Nature* **400**, 167 (1999).
27. N. R. J. Glossop, L. C. Lyons, P. E. Hardin, *Science* **286**, 766 (1999).
28. H. Tei et al., *Nature* **389**, 512 (1997).
29. L. P. Shearman, M. J. Zylka, S. M. Reppert, D. R. Weaver, *Neuroscience* **89**, 387 (1999).
30. S. Honma, M. Ikeda, H. Abe, Y. Tanahashi, M. Namihira, *Biochem. Biophys. Res. Commun.* **250**, 83 (1998).
31. K. Oishi, K. Sakamoto, T. Okada, T. Nagase, N. Ishida, *Biochem. Biophys. Res. Commun.* **253**, 199 (1998).
32. Semiquantitative in situ hybridization with radioactive cRNA probes was performed as described (12).
33. W. Yu et al., *Biochem. Biophys. Res. Commun.* **260**, 760 (1999).
34. The probe for *Bmal1* was from nucleotides 864 to 1362 of mouse *Bmal1b* (GenBank accession number AF015203).
35. M. J. Zylka, L. P. Shearman, D. R. Weaver, S. M. Reppert, *Neuron* **20**, 1103 (1998).
36. A breeding colony of mice carrying the *Clk* mutation on a BALB/c genetic background was established from mice provided by M. H. Vitaterna and J. S. Takahashi. Sex ratios of male and female mice were balanced across time points. Animal studies at Massachusetts General Hospital were approved by the Subcommittee on Research Animal Care.
37. The colony of mice carrying the *mPer2^{brdm1}* mutation was established on a C57BL/6 × 129SvEvBrd hybrid background (26). Balanced sex ratios of male and female mice were used.
38. B. Zheng et al., unpublished data.
39. L. P. Shearman, X. Jin, S. M. Reppert, D. R. Weaver, unpublished data.
40. COS-7 cells (3×10^5) were seeded on glass cover slips in six-well dishes and transfected with Lipofectamine Plus (Gibco BRL) with 0.5 μ g of total DNA per well. Forty-eight hours after transfection, cells were processed as described (13). A random population of 30 to 60 cells from each cover slip was examined by epifluorescence microscopy, and the subcellular distribution of expressed proteins was recorded without knowledge of treatment. At least three independently transfected cover slips were analyzed.
41. L. P. Shearman et al., data not shown.
42. L. P. Shearman, M. J. Zylka, D. R. Weaver, L. F. Kolakowski Jr., S. M. Reppert, *Neuron* **19**, 1261 (1997).
43. The *mCry*-deficient (double mutant) colony of mice had a C57BL/6 × 129 hybrid background, and wild-type controls were of the same genetic background (24). Sex ratios of male and female mice were balanced across time points.
44. E. Vielhaber, E. Eidi, A. Rivers, Z.-H. Gao, D. M. Virshup, *Mol. Cell. Biol.*, in press.
45. L. Saez and M. W. Young, *Neuron* **17**, 911 (1996).
46. T. K. Darlington et al., *Science* **280**, 1599 (1998).
47. 52 cells were transfected with Cellfectin (Gibco BRL). Each transfection consisted of 10 to 100 ng of expression plasmid with indicated inserts in pACS.1-V5, 10 ng of luciferase reporter, and 25 ng

- of β -galactosidase (β -Gal) internal control plasmid (driven by baculovirus immediate-early gene, *ie-1* promoter). Total DNA for each transfection was normalized with pAC5.1-V5. Cells were harvested 48 hours after transfection. Luciferase activity was normalized by determining luciferase: β -Gal activity ratios and averaging the values from triplicate wells.
48. M. F. Ceriani *et al.*, *Science* **285**, 553 (1999).
49. MOP4 is a basic helix-loop-helix, PAS-containing transcription factor that is closely related to CLOCK.

- It can also heterodimerize with BMAL1 to activate transcription through E box enhancers (10, 13).
50. DNA binding constructs were made as LexA (1-202) fusions. VP-16 transactivator hybrids were generated in pVP-16. Two-hybrid assays were performed as described [N. Gekakis *et al.*, *Science* **270**, 811 (1995)].
51. E. A. Griffin, D. Staknis, C. J. Weitz, *Science* **286**, 768 (1999).
52. Luciferase reporter gene assays were performed in COS-7 cells as described (12).
53. G. A. Keesler *et al.*, *Neuroreport* **11**, 951 (2000).

54. P. L. Lowrey *et al.*, *Science* **288**, 483 (2000).
55. We thank S. Kay and C. Weitz for expression and reporter constructs and A. Chavda and C. Capodice for technical support. Supported by R37 HD14427 and RO1 NS39303, BBSRC 8/S09882, and a Spinoza Premium of the Netherlands Organization for Scientific Research. L.P.S. was supported in part by NIH Training Grant HL07901, K.K. by the University of Tokyo, and C.C.L. by the NIH.

15 March 2000; accepted 13 April 2000

Earliest Pleistocene Hominid Cranial Remains from Dmanisi, Republic of Georgia: Taxonomy, Geological Setting, and Age

Leo Gabunia,¹ Abesalom Vekua,¹ David Lordkipanidze,^{2*} Carl C. Swisher III,^{3†} Reid Ferring,⁴ Antje Justus,⁵ Medea Nioradze,² Merab Tvalchrelidze,² Susan C. Antón,⁶ Gerhard Bosinski,⁵ Olaf Jöris,⁵ Marie-A.-de Lumley,⁷ Givi Majsuradze,² Aleksander Mouskhelishvili²

Archaeological excavations at the site of Dmanisi in the Republic of Georgia have uncovered two partial early Pleistocene hominid crania. The new fossils consist of a relatively complete cranium and a second relatively complete calvaria from the same site and stratigraphic unit that yielded a hominid mandible in 1991. In contrast with the uncertain taxonomic affinity of the mandible, the new fossils are comparable in size and morphology with *Homo ergaster* from Koobi Fora, Kenya. Paleontological, archaeological, geochronological, and paleomagnetic data from Dmanisi all indicate an earliest Pleistocene age of about 1.7 million years ago, supporting correlation of the new specimens with the Koobi Fora fossils. The Dmanisi fossils, in contrast with Pleistocene hominids from Western Europe and Eastern Asia, show clear African affinity and may represent the species that first migrated out of Africa.

The identity of the first hominid species to disperse out of Africa and the timing of this dispersal remain highly controversial. The earliest known hominid fossils in Europe and Asia have either exhibited morphological characteristics specific to the region in which they were found (1, 2) or were too incomplete to be identified reliably as to species (3, 4). Thus, it is debatable whether any of these earliest ex-African hominids are conspecific with those from

Africa. Equally debatable are the timing and cause of the first hominid dispersal outside of Africa. Few sites of critical age have yielded both significant hominid remains and artifacts from geological contexts that are amenable to reliable dating. Thus, it remains debated whether hominids dispersed from Africa in the late Pliocene to early Pleistocene, before the development of Acheulean tool technologies, or much later in the middle Pleistocene at or after 1 million years ago (Ma), well after the development of these technologies (5). Advocates of a post-1.0 Ma dispersal time have suggested that technological innovation, as witnessed by the Acheulean tradition, enabled hominid dispersal from Africa (6), whereas an earlier, pre-Acheulean dispersal supports a more ecomorphological web of factors as the cause of hominid dispersal (7, 8).

Recent discoveries at Dmanisi in the Republic of Georgia (Fig. 1) provide us with a data set with which to evaluate these scenarios. Archaeological excavations at Dmanisi during the summer of 1999 produced two hominid crania, D2280 (Fig. 2) and D2282

(Fig. 3) from the same stratigraphic level and excavation pit as a hominid mandible discovered in 1991 (3, 9), for which the taxonomic affinity is debated (3, 6, 10, 11). Here we describe the new hominid fossils; their taxonomic affinity; and age, geological context, associated artifacts, and vertebrate fauna.

The new fossils. The first fossil specimen, D2280 (Fig. 2), is an almost complete calvaria, including a partial cranial base retaining slightly damaged nuchal and basilar portions of the occipital, parts of the greater wings of the sphenoid, and most of the left mandibular fossa of the temporal. The second and more complete is cranium D2282 (Fig. 3), which retains much of the face and cranial vault but has undergone lateral and dorsoventral postmortem deformation. The occipital and temporal regions are crushed on the left side, as are the zygomatic bones. The base is largely absent. Much of the median upper facial skeleton is missing, including the supraorbital torus at glabella, nasal bones, and frontal processes of the maxillae. However, the maxillae are well preserved laterally and inferiorly and retain the slightly worn right P⁴-M², the left M¹ and M², and the alveoli of all other adult teeth, including those of M³, which are visible on radiograph. D2282 is the smaller of the two, and based on gracile muscle attachments, less well-developed cranial superstructures, light dental wear, and well-demarcated cranial sutures, may be either an older subadult or young adult and possibly a female.

Both specimens are small with endocranial volumes below 800 cm³ (Tables 1 and 2). A direct measurement using seed yielded an endocranial volume of 775 cm³ for D2280. The cranial capacity estimate calculated from the length, breadth, and cranial index of D2282 is about 650 cm³.

Cranial shape is similar in both specimens: spheroidal in superior view and relatively low and angular in lateral view (Figs. 2 and 3). The greatest cranial breadth is at the level of the well-pneumatized mastoid processes. The occipitals are relatively narrow and angular. The occipital angle in D2280 is 108°. A continuous occipital torus is present in each specimen, and D2280 exhibits a larger torus and more rugose nuchal muscle markings than does D2282. A pronounced occipital crest extends from the external occipital protuberance to the foramen magnum in D2280. The frontal sinus and ethmoid pneumatization are visible in D2280. A

¹Republic of Georgia National Academy of Sciences, Tbilisi, 380007, Republic of Georgia. ²Department of Geology and Paleontology, Republic of Georgia State Museum, 3 Purtseladze Street, Tbilisi, 380007, Republic of Georgia. ³Berkeley Geochronology Center, 2455 Ridge Road, Berkeley, CA 94709, USA. ⁴Department of Geography, University of North Texas, Denton, TX 76203, USA. ⁵Romisch-Germanisches Zentralmuseum, Mainz, Germany. ⁶Department of Anthropology, University of Florida, Gainesville, FL 32611, USA. ⁷Laboratoire Muséum National d'Histoire Naturelle, CNRS, Paris, France.

*To whom correspondence should be addressed. E-mail: geonathist@ip.osgf.ge

†To whom reprint requests should be addressed. E-mail: cswish@bgc.org